

## Transport properties of Cu-O chains in $\text{Sr}_2\text{CuO}_{3+\delta}$

W. B. Archibald, J.-S. Zhou, and J. B. Goodenough

Center for Materials Science and Engineering, ETC 9.102, University of Texas at Austin, Austin, Texas 78712-1063

(Received 10 July 1995)

High-pressure oxidation of  $\text{Sr}_2\text{CuO}_{3+\delta}$  with  $\delta < 0.1$  has produced samples with metallic chains as well as those with small-polaron behavior. The paramagnetic susceptibility evolves with increasing  $\delta$  from a primarily Bonner-Fisher temperature dependence to a Curie-Weiss behavior for small-polaron samples and a strongly mass-enhanced Pauli paramagnetism for the metallic samples. Samples of intermediate oxidation exhibited a smooth transition from metallic behavior at low temperatures to small-polaron behavior at higher temperatures. The small low-temperature Seebeck coefficient  $\alpha(T)$  of the metallic samples exhibited a negative enhancement characterized by a hump at approximately 75 K typical of acoustic-phonon drag; there was no evidence for an  $\alpha(T)$  like that of the  $\text{CuO}_2$  planes of the superconductive cuprates, which have an enhancement with a  $T_{\text{max}} \approx 140$  K that we have associated with vibronic states derived from dynamic pseudo-Jahn-Teller deformations of the Cu sites inside large correlation polarons. These data support the suggestion that an enhancement with a  $T_{\text{max}} \approx 140$  K found for the chains in  $\text{YBa}_2\text{Cu}_3\text{O}_{6.96}$  is the result of a strong elastic coupling to the superconductive  $\text{CuO}_2$  sheets and is not an intrinsic property of the chains.

### INTRODUCTION

We report on the transport properties of orthorhombic  $\text{Sr}_2\text{CuO}_{3+\delta}$ , which contains isolated chains of corner-shared square-coplanar  $\text{CuO}_4$  units (Fig. 1). Similar one-dimensional chains are found in the 90-K superconductor  $\text{YBa}_2\text{Cu}_3\text{O}_{7-\delta}$ , but in this structure the apical oxygen are shared by the Cu of the superconductive two-dimensional  $\text{CuO}_2$  sheets. In superconductive  $\text{La}_{2-x}\text{Sr}_x\text{CuO}_4$ , there are no chains, only  $\text{CuO}_2$  sheets.

In the superconductive and overdoped  $\text{La}_{2-x}\text{Sr}_x\text{CuO}_4$

compositions, we have found<sup>1</sup> an enhancement term  $\delta\alpha(T)$  in the Seebeck coefficient

$$\alpha(T) = \alpha_0 + \delta\alpha(T), \quad (1)$$

that has a maximum value at a  $T_{\text{max}} \approx 140$  K; the nearly temperature-independent term  $\alpha_0$  decreases monotonically from a large, positive value in the optimally doped sample  $x=0.15$  to a small, negative value in the overdoped sample  $x=0.30$ . We have argued that a  $T_{\text{max}} \approx 140$  K is too high for the  $\delta\alpha(T)$  enhancement to be accounted for with a process involving acoustic phonons, but that it is compatible with one involving optical-mode phonons. We have also shown that holes trapped in pockets of more covalently bonded regions of a  $\text{CuO}_2$  sheet would form nonadiabatic large polarons occupying about five Cu sites as a result of cooperative, dynamic pseudo-Jahn-Teller deformations of the sites within a polaron,<sup>2,3</sup> and that inter-polaron elastic coupling would cause the polaron gas to condense into a polaron liquid below 300 K and into a polaron solid below  $T_C$  in the superconductive compositions.<sup>2-4</sup> The strong electron-lattice interactions associated with the dynamic, cooperative pseudo-Jahn-Teller deformations result in vibronic charge carriers that, as a polaron-liquid or polaron-solid phase, give rise to a vibronic energy dispersion  $\epsilon(\mathbf{k})$  capable of introducing an optical-mode enhancement  $\delta\alpha(T)$  to the Seebeck coefficient. Moreover, the vibronic energy dispersion  $\epsilon(\mathbf{k})$  would be extremely flat in the Cu-O bond directions, as observed with angle-resolved photoemission spectroscopy,<sup>5</sup> and would exhibit a midband energy gap in the superconductive compositions that disappeared with the loss of polaron formation in the overdoped compositions where the vibronic states become homogeneous over the Cu atoms of a  $\text{CuO}_2$  sheet.

Thermopower measurements of the  $\text{YBa}_2\text{Cu}_3\text{O}_{7-\delta}$  90-K superconductor record a negative contribution from the chains of the  $\text{Cu}(1)\text{O}_{1-\delta}$  planes that is competitive with the

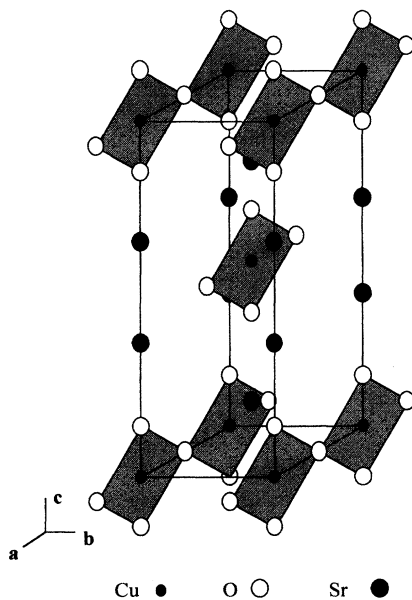


FIG. 1. The structure of orthorhombic  $\text{Sr}_2\text{CuO}_3$  showing isolated chains of corner-shared square-coplanar  $\text{CuO}_4$  units.

positive contribution from the  $\text{CuO}_2$  sheets.<sup>6</sup> By simultaneously substituting Ca for Y and La for Ba so as to maintain the optimum oxidation state of the Cu-O array, it proved possible to suppress the chain contribution to the thermopower by breaking up the chains.<sup>7</sup> With this strategy we could demonstrate not only that the optimally doped  $\text{CuO}_2$  sheets gave the same thermopower behavior in  $\text{YBa}_2\text{Cu}_3\text{O}_{7-\delta}$  as in  $\text{La}_{2-x}\text{Sr}_x\text{CuO}_4$ , but also that the chain contribution too could be described by Eq. (1), but with a change in sign of both  $\alpha_0$  and  $\delta\alpha(T)$  with a  $T_{\text{max}} \approx 140$  K as for the sheets. Since the chains would not support vibronic states associated with cooperative pseudo-Jahn-Teller deformations as in the  $\text{CuO}_2$  sheets unless they were driven by coupling to the sheets, we were motivated to investigate the character of the charge carriers in isolated chains and whether any enhancement associated with itinerant charge carriers in these chains gave an enhancement factor  $\delta\alpha(T)$  with a  $T_{\text{max}} \approx 140$  K or one with a lower  $T_{\text{max}}$  characteristic of a conventional acoustic-phonon drag.

The isolated Cu-O chains of the orthorhombic  $\text{Sr}_2\text{CuO}_3$  structure, Fig. 1, give a spin magnetic susceptibility described by<sup>8</sup>

$$\chi(T) = \rho\chi_{\text{CW}} + (1 - \rho)\chi_{\text{BF}}, \quad (2)$$

where  $\chi_{\text{CW}}$  is a Curie-Weiss component associated with impurities or short chain lengths with an odd number of  $\text{Cu}^{2+}$  sites and  $\chi_{\text{BF}}$  is the Bonner-Fisher<sup>9</sup> susceptibility for an  $S=1/2$  infinite, isotropic Heisenberg chain with an antiferromagnetic exchange constant  $|J|/k_B \approx 1300$  K. The low-spin  $\text{Cu}^{3+}$  centers are diamagnetic. The parameter  $\rho$  increased with oxidation, but the extent of doping of the chains either  $n$ -type or  $p$ -type has been so small that there has been no report on their transport properties. A challenge for us, therefore, was to find a way to oxidize the chains sufficiently to render them metallic; without an energy dispersion  $\epsilon(\mathbf{k})$ , it would not be possible to observe an enhancement term  $\delta\alpha(T)$  of the Seebeck coefficient.<sup>1</sup> However, the experiment faced another hazard. A one-dimensional metal having a partially filled, narrow band of itinerant electrons is unstable with respect to stabilization of a Peierls charge-density wave (CDW) in a single-valent system and to a sliding CDW in a mixed-valent system.

Fortunately we have been able to oxidize under high oxygen pressure the Cu-O chains to the metallic state with no CDW transition; the thermopower shows a  $\delta\alpha(T)$ , but with a  $T_{\text{max}} \approx 75$  K characteristic of a conventional phonon drag rather than the  $T_{\text{max}} \approx 140$  K characteristic of the superconductive copper oxides.

## EXPERIMENTAL

$\text{Sr}_2\text{CuO}_3$  was prepared by conventional solid-state reaction of stoichiometric quantities of  $\text{SrCO}_3$  and  $\text{CuO}$  calcined at  $950^\circ\text{C}$ , sintered at  $1000^\circ\text{C}$  in air, and quenched from  $500^\circ\text{C}$ . We were unable to make  $n$ -type  $\text{Sr}_2\text{CuO}_3$  with either chemical substitution or reduction under high pressure. However, we were able to oxidize  $\text{Sr}_2\text{CuO}_3$  under a high oxygen pressure in the range  $20 \leq P_{\text{O}(2)} \leq 55$  kbar at temperatures  $800 \leq T \leq 1100^\circ\text{C}$ .

Powdered single-phase  $\text{Sr}_2\text{CuO}_3$  was pelletized, sintered, and placed in a copper crucible together with  $\text{KClO}_4$  as an

oxygen source. A gold ring was placed between the sample and the copper crucible; a disk of yttrium-stabilized zirconia separated the sample and the  $\text{KClO}_4$ . The zirconia disk allowed the transfer of oxygen, but blocked the transfer of  $\text{K}^+$  and  $\text{Cl}^-$  ions. Separation of the sample and the  $\text{KClO}_4$  proved critical as contamination with  $\text{K}^+$  ions stabilizes an  $\text{Sr}_2\text{CuO}_{4-\lambda}$  tetragonal phase containing  $\text{CuO}_2$  planes. Before assembly, all materials were dried. The temperature inside the pressure chamber was determined from a calibrated curve of heater-input power versus temperature. The interstitial-oxygen concentration of the product could be controlled by varying the temperature of the high-pressure anneal. All samples were quenched under high pressure. Oxidized  $\text{Sr}_2\text{CuO}_{3+\delta}$  samples exhibiting polaronic transport behavior were highly reproducible; the preparation of metallic samples was more difficult to reproduce as the synthesis conditions are very close to those that transform the orthorhombic phase to the tetragonal phase containing  $\text{CuO}_2$  planes instead of chains.

Previous attempts<sup>10</sup> to prepare orthorhombic  $\text{Sr}_2\text{CuO}_{3+\delta}$  missed the orthorhombic phase with metallic chains because of stabilization of the tetragonal phase under high pressure. In those experiments, there was contact of the sample with the  $\text{KClO}_4$  oxygen source. We found that such contact converts the orthorhombic  $\text{Sr}_2\text{CuO}_{3+\delta}$  phase to the tetragonal phase at lower annealing temperatures, which narrows the range of  $\delta$  for the orthorhombic phase in the  $P$ - $T$  phase diagram and suppresses the metallic compositions.

All the orthorhombic  $\text{Sr}_2\text{CuO}_{3+\delta}$  samples, both those having polaronic conduction and those that were metallic, gradually lose oxygen over a period of a few days under ambient conditions. Therefore all measurements were carried out on fresh samples below  $300$  K.

Since the  $\text{Sr}_2\text{CuO}_{3+\delta}$  structure lacks high-angle diffraction peaks, we calculated the lattice parameters by curve fitting several good-profile peaks against Mo as an internal standard. The oxygen content was determined by iodometric titration. Magnetic susceptibilities were taken with a superconducting quantum interference device magnetometer (Quantum Design); thermopower and conductivity data were obtained with a home-built apparatus described elsewhere.<sup>11</sup>

In the metallic samples the value of the Seebeck coefficient is low enough that the contribution from the copper leads cannot be neglected, especially in the low-temperature range. In order to correct for the background, the contribution to the Seebeck coefficient from the copper leads was measured directly at low temperatures ( $T < 80$  K) with a 123-superconductor sample. The copper-lead contribution above  $80$  K is almost linearly dependent on temperature and was taken from the literature.

## RESULTS

From Fig. 1, it is apparent that the extra oxygen can occupy two possible interstitial sites: one is located between two Cu atoms of adjacent Cu-O chains, the other is within the  $\text{Sr}_2\text{O}_2$  rocksalt layer coordinated tetrahedrally by four  $\text{Sr}^{2+}$  ions and also by four oxygen atoms as in  $\text{La}_2\text{NiO}_{4+\delta}$  (Ref. 12) and  $\text{La}_2\text{CuO}_{4+\delta}$ .<sup>13</sup> The evolution of the lattice parameters with increasing interstitial oxygen concentration  $\delta$  is given in Table I; an increase in the  $c$  parameter with no

TABLE I. Lattice parameters and additional oxygen content ( $\delta$ ) for the metallic, polaronic, and as-prepared  $\text{Sr}_2\text{CuO}_{3+\delta}$ .

	As-prepared	Polaronic	Metallic
$a$ (Å)	3.916(0)	3.917(1)	3.915(2)
$b$ (Å)	3.502(1)	3.500(1)	3.499(1)
$c$ (Å)	12.706(2)	12.713(2)	12.712(2)
$\delta$	0.01(1)	0.03(1)	$0.03 < \delta < 0.1^a$

<sup>a</sup>The oxygen content of the metallic phase is uncertain due to the small sample size.

measurable change in the  $a$  and  $b$  parameters indicates that the interstitial oxygen atoms occupy sites in the  $\text{Sr}_2\text{O}_2$  rock-salt layers. In the  $\text{Sr}_2\text{O}_2$  layers, the interstitial oxygen does not coordinate a Cu atom, so the Cu-O-Cu interactions in the chains remain relatively unperturbed except for interactions between the interstitial oxygen and the apical oxygen of the chains. In the case of  $\text{La}_2\text{CuO}_{4+\delta}$ , the interstitial oxygen oxidize the  $\text{CuO}_2$  sheets at low temperatures to make them superconductive.<sup>14</sup> Similarly located interstitial oxygen atoms in  $\text{Sr}_2\text{CuO}_{3+\delta}$  can be expected to oxidize the Cu-O chains by capturing two electrons to become  $\text{O}_i^{2-}$  ions rather than bonding with the apical oxygen to form a polyanion such as the peroxide ( $\text{O}_2$ )<sup>2-</sup> ion.

Figure 2 shows the x-ray-diffraction patterns taken with Cu  $K\alpha$  radiation in the range  $30.5^\circ \leq 2\theta \leq 35^\circ$  for (a) the lightly oxidized (polaronic) and the parent orthorhombic

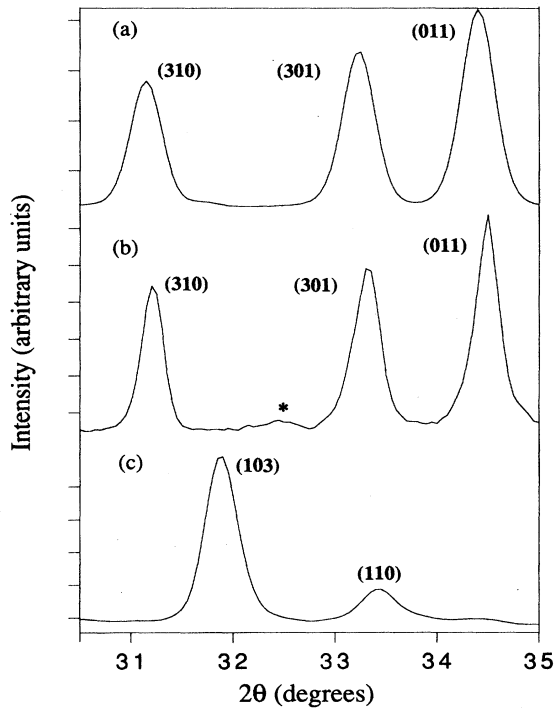


FIG. 2. Evolution of the x-ray-diffraction pattern with doping in the range  $30.5^\circ \leq 2\theta \leq 34^\circ$ . (a) As-prepared and lightly oxidized (polaronic), orthorhombic  $\text{Sr}_2\text{CuO}_{3+\delta}$ , (b) metallic, orthorhombic  $\text{Sr}_2\text{CuO}_{3+\delta}$  with superlattice peak marked with (\*), (c) tetragonal  $\text{Sr}_2\text{CuO}_{4-\lambda}$ .

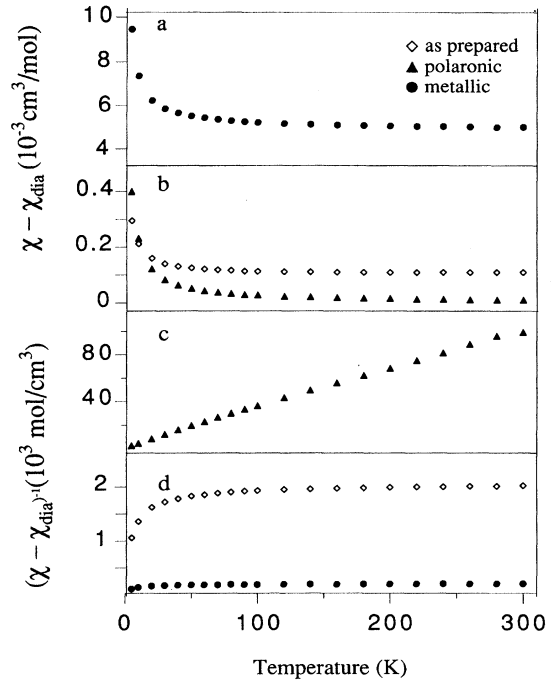


FIG. 3. Magnetic susceptibility ( $\chi$ ) and inverse magnetic susceptibility ( $\chi^{-1}$ ) vs temperature with diamagnetic core contributions ( $\chi_{\text{dia}}$ ) subtracted.

$\text{Sr}_2\text{CuO}_{3+\delta}$ , (b) the metallic, orthorhombic  $\text{Sr}_2\text{CuO}_{3+\delta}$ , and (c) the tetragonal phase. The metallic samples show a superlattice peak at  $2\theta \approx 32.3^\circ$ ; this peak does not belong to the tetragonal phase, which has a peak below  $2\theta = 32^\circ$ . We presume the superlattice peak is due to an ordering of the interstitial oxygen atoms.

Ami *et al.*<sup>8</sup> found the Curie-Weiss component in Eq. (2) increases with  $\delta$  (to a maximum  $\delta \approx 0.02$  in their experiments), which they interpreted to be due to an increase of finite chain lengths containing an odd number of  $\text{Cu}^{2+}$  ions. Figure 3 shows our spin susceptibility data obtained by subtracting from the measured susceptibility a closed-shell diamagnetic term  $\chi_{\text{dia}} = -7.7 \times 10^{-5} \text{ cm}^3/\text{mol}$ . For the starting material, a small value of the parameter  $\rho$  of Eq. (2) indicates a nearly stoichiometric  $\text{Sr}_2\text{CuO}_3$  according to the analysis of Ami *et al.*<sup>8</sup> As  $\delta$  increases in orthorhombic, polaronic  $\text{Sr}_2\text{CuO}_{3+\delta}$ , creation of low-spin  $\text{Cu}^{3+}$  ions reduces the lengths of the spin-1/2 antiferromagnetic chains, and the Curie-Weiss component increases until a typical Curie-Weiss behavior is found as illustrated in Figs. 3(b) and 3(c). However, oxidation to metallic, orthorhombic  $\text{Sr}_2\text{CuO}_{3+\delta}$  destroys the Curie-Weiss behavior; the metallic phase shows a nearly temperature-independent magnetic susceptibility, Fig. 3, that is higher than expected for a conventional metal. The high density of states at the Fermi energy  $\epsilon_f$  derived from an itinerant-particle model indicates a strong mass enhancement of the Pauli susceptibility. The itineracy of the electronic states in the metallic samples is confirmed by the thermopower data shown in Fig. 4.

As Figs. 4 and 5 show, the starting  $\text{Sr}_2\text{CuO}_3$  sample gives a typical semiconductive behavior expected for a half-filled

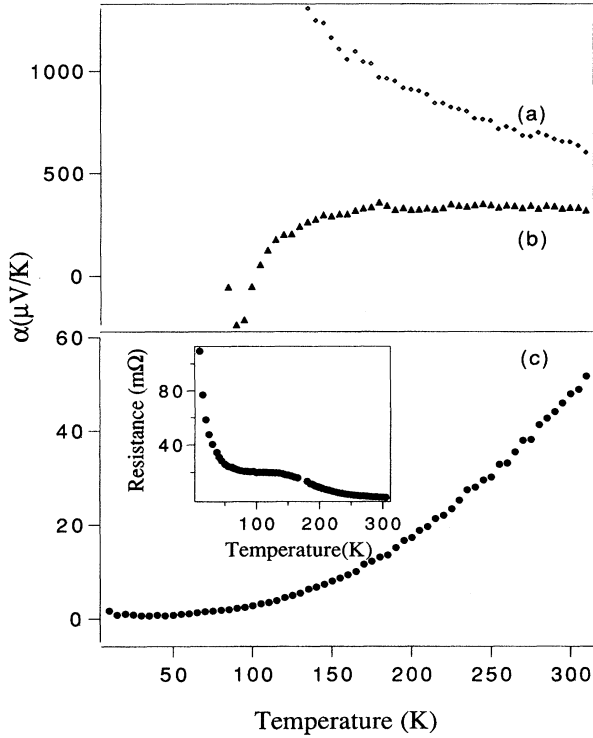


FIG. 4. Seebeck coefficient  $\alpha$  vs temperature for (a) as-prepared, (b) polaronic, and (c) metallic  $\text{Sr}_2\text{CuO}_{3+\delta}$ . Inset: Resistance vs temperature for the metallic sample.

$z^2-x^2$  band that is split into two Hubbard bands by strong on-site electron-electron interactions. Charge carriers are introduced by thermal excitation across an energy gap. The large  $\chi_{\text{BF}}$  in this sample is consistent with this result. The lightly doped  $\text{Sr}_2\text{CuO}_{3+\delta}$  samples show a large, temperature-independent Seebeck coefficient above 200 K that is typical of polaronic behavior. Calculation of the magnitude of  $\alpha = (k/e) \ln [2(1-c)/c]$  for a small-polaron occupancy frac-

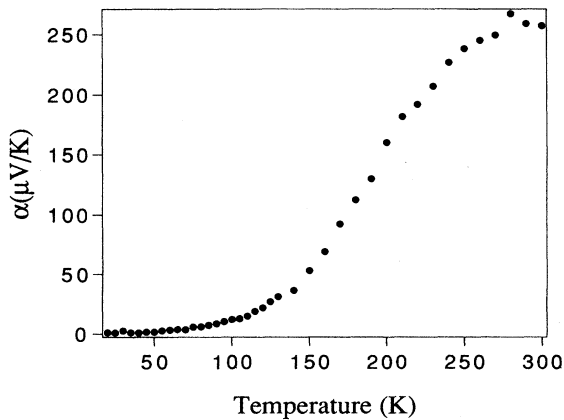


FIG. 5. Seebeck coefficient  $\alpha$  vs temperature for a sample with oxygen doping intermediate to the metallic and polaronic samples of Fig. 4 showing a smooth transition from metallic behavior at low temperatures to small-polaron behavior at higher temperatures.

tion  $c$  gave a value for  $c$  equal, within experimental error, to  $2\delta$  as determined by iodometric titration. A small-polaron hopping conduction of holes at low-spin  $\text{Cu}^{3+}$  ions is also consistent with our interpretation of the evolution of magnetic susceptibility with  $\delta$ .

The metallic sample of Fig. 4 gave a small Seebeck coefficient that increases nearly linearly with temperature below and above 200 K. The inset of Fig. 4 shows there is also a resistivity anomaly at 200 K. Another sample, Fig. 5, shows metallic behavior below 120 K with a transition to polaronic behavior above 230 K. The data of Figs. 4 and 5 are corrected by subtraction of the contribution from the copper leads as determined independently. In addition to the change in slope of  $\alpha(T)$  near 200 K, we call attention to two additional features of Fig. 4: the high values of  $\alpha(T)$  above 200 K and a negative enhancement factor  $\delta\alpha(T)$  below 200 K with a hump centered at  $T_{\text{max}} \approx 75$  K.

## DISCUSSION

The Cu-O bond lengths in orthorhombic  $\text{Sr}_2\text{CuO}_3$  have an equilibrium value for a  $\text{Cu}^{2+}$  ion, which makes it difficult to add or subtract antibonding electrons within this structure. As demonstrated for  $\text{CuO}_2$  sheets,<sup>15</sup> application of a tensile stress is needed for  $n$ -type doping and of a compressive stress for  $p$ -type doping. We were able to dope orthorhombic  $\text{Sr}_2\text{CuO}_3$   $p$ -type by oxidation under a compressive stress with  $P_{\text{O}(2)} \leq 55$  kbar to obtain  $\text{Sr}_2\text{CuO}_{3+\delta}$  with  $\delta < 0.1$ . Application of higher oxygen pressures or substitution of some  $\text{Sr}^{2+}$  by  $\text{K}^+$  stabilizes a tetragonal  $\text{Sr}_2\text{CuO}_{4-\lambda}$  phase containing  $\text{CuO}_2$  planes with Cu atoms coordinated by five or six oxygen atoms.

In orthorhombic  $\text{Sr}_2\text{CuO}_{3+\delta}$  the  $\delta$  excess oxygen atoms occupy interstitial sites in the  $\text{Sr}_2\text{O}_2$  sheets as  $\text{O}_i^{2-}$  ions, a situation analogous to that of the  $\delta$  excess oxygen in  $\text{La}_2\text{NiO}_{4+\delta}$  and superconductive  $\text{La}_2\text{CuO}_{4+\delta}$ . The appearance of a superlattice diffraction peak in metallic  $\text{Sr}_2\text{CuO}_{3+\delta}$  samples suggests an ordering of the  $\text{O}_i^{2-}$  ions.

As in the  $\text{CuO}_2$  sheets of the cuprate superconductors, there is a change from small-polaron to metallic (large-polaron) conduction with increased oxidation. However, the  $\text{CuO}_2$  sheets have intermediate-size nonadiabatic polarons (about five Cu sites) and a condensation of a polaron gas into a polaron liquid segregating the parent antiferromagnetic-insulator phase from the superconductive phase below 300 K in the underdoped region; the isolated chains of  $\text{Sr}_2\text{CuO}_{3+\delta}$  support only small polarons (one Cu site) or a metallic behavior characteristic of a mass-enhanced Fermi liquid. The smooth transition from Fermi-liquid (or large-polaron) to small-polaron behavior with increasing temperature at intermediate doping, Fig. 5, contrasts sharply with the transition from a polaron liquid to a polaron gas near 300 K in the superconductive cuprates. In the superconductors, a  $\delta\alpha(T)$  with a  $T_{\text{max}} \approx 140$  K is superposed on a large  $\alpha_0$  whereas the isolated chains of metallic  $\text{Sr}_2\text{CuO}_{3+\delta}$  have a small  $\alpha(T)$  at lower temperatures with a  $\delta\alpha(T) < 0$  described by a hump with a broad maximum at  $T_{\text{max}} \approx 75$  K, which is typical of a phonon-drag process,<sup>16</sup> but with the peak greatly suppressed. There is no evidence for vibronic coupling in isolated chains; the  $\delta\alpha(T)$  with a  $T_{\text{max}} \approx 140$  K observed for chains in the

90-K superconductor  $\text{YBa}_2\text{Cu}_3\text{O}_{7-\delta}$  is therefore to be associated with a strong elastic coupling in that compound to  $\text{CuO}_2$  sheets where, we have postulated, vibronic coupling is occurring within the polarons of a polaron liquid to give a vibronic energy dispersion  $\epsilon(\mathbf{k})$ . The elastic coupling between chains and sheets via shared apical oxygen atoms provides a coupling mechanism between  $\text{CuO}_2$  sheets across the  $\text{Cu}(1)\text{O}_{1-\delta}$  planes that may be as important as the band overlap of the charge reservoir in contributing to the high- $T_c$  of  $\text{YBa}_2\text{Cu}_3\text{O}_{7-\delta}$ .

The Seebeck coefficient for polaronic conduction obeys the hopping formula  $\alpha=(k/e)\ln[2(1-c)/c]$  only in the high-temperature limit, which corresponds to  $T>150$  K in Fig. 4(b). At low temperatures, the Seebeck coefficient normally approaches zero as  $T^{1/2}$ . However, polaronic  $\text{Sr}_2\text{CuO}_{3+\delta}$  shows an abrupt drop in  $\alpha$  to a negative value below 150 K, Fig. 4(b), which we associate with the onset of either a static charge-density wave or long-range ordering of  $\text{Cu}^{3+}$  ions. Therefore, the absence of a CDW in metallic  $\text{Sr}_2\text{CuO}_{3+\delta}$  is noteworthy.

The linear relation between  $\alpha$  and temperature found in the metallic samples is expected from the Mott formula; the additional hump at low temperatures ( $T_{\text{max}}\approx 75$  K) is due to phonon drag. The magnitude of the thermopower of a metal at a given temperature reflects the asymmetry of the  $\epsilon(\mathbf{k})$  dispersion curve near the Fermi energy  $\epsilon_f$ ; the value of  $\alpha$  is normally below  $40 \mu\text{V}/\text{K}$ , so the high value of  $\alpha$  above 200 K in Fig. 4(c) is exceptional. The extremely high value of the susceptibility in our metallic  $\text{Sr}_2\text{CuO}_{3+\delta}$  indicates a narrow-band conduction at the limit where a transition to polaronic behavior occurs. As the temperature increases at this limit, motional narrowing could cause a resonance between the itinerant and small-polaron electron states with a full transition to small-polaron conduction at higher temperatures. Just such a transition is seen below 300 K in Fig. 5, and we believe that the change in the slope of the Seebeck coefficient above  $20 \mu\text{V}/\text{K}$  in Fig. 4(c) reflects the onset of such a transition in our metallic  $\text{Sr}_2\text{CuO}_{3+\delta}$  sample. In this case  $\alpha$  no longer possesses a pure itinerant behavior. The anomaly in the resistance measurement seems to support this argument. Although the resistance of this one-dimensional sys-

tem is dominated by grain-boundary scattering, nevertheless the temperature-independent resistance changes to semiconductive behavior around 180 K, which corresponds to the change in slope in the thermopower vs temperature. We suspect that the phonon drag is associated with a large itinerant electron fraction, but that a resonance to a small-polaron fraction persists to lowest temperatures to suppress stabilization of a CDW and phonon drag in this phase.

## CONCLUSIONS

Orthorhombic  $\text{Sr}_2\text{CuO}_3$  exhibiting Bonner-Fisher behavior was doped under high oxygen pressure. Orthorhombic  $\text{Sr}_2\text{CuO}_{3+\delta}$  shows semiconducting, small-polaron, and metallic conduction as  $\delta$  is increased. Comparison of the magnetic and transport behavior of orthorhombic  $\text{Sr}_2\text{CuO}_{3+\delta}$  and the  $\text{CuO}_2$  sheets of the cuprate superconductors indicates that the cooperation of lattice deformations associated with the charge carriers in two dimensions is a necessary condition for the formation of intermediate-size polarons. Metallic  $\text{Sr}_2\text{CuO}_{3+\delta}$  exhibits normal phonon-drag effects with a peak at  $T_{\text{max}}\approx 75$  K instead of the large enhancement in  $\alpha(T)$  at  $T_{\text{max}}\approx 140$  K found in the cuprate superconductors, which we have interpreted as evidence for vibronic coupling between optical phonons and electronic states. A smooth transition from metallic to polaronic behavior with increasing temperature suggests the coexistence of the two types of electrons is present over a wide temperature range and may be responsible for suppressing a Peierls distortion and the phonon-drag component in the thermopower of the metallic chains.

*Note added in proof.* Shin *et al.*<sup>17</sup> have reported an investigation of  $\text{Sr}_{2-x}\text{Na}_x\text{CuO}_3$  ( $0\leq x\leq 0.5$ ). This system remains a polaronic conductor to  $x=0.5$ .

## ACKNOWLEDGMENTS

We would like to thank Dr. K. S. Nanjundaswamy for his help in sample preparation, and the Robert A. Welch Foundation, Houston, Texas, the Texas Advanced Research Program, and the National Science Foundation for financial support.

<sup>1</sup>J.-S. Zhou and J. B. Goodenough, Phys. Rev. B **51**, 3104 (1995).

<sup>2</sup>G. Bersuker and J. B. Goodenough (unpublished).

<sup>3</sup>J.-S. Zhou, G. Bersuker, and J. B. Goodenough, J. Supercond., **8** (1995).

<sup>4</sup>J. B. Goodenough and J.-S. Zhou, Phys. Rev. B **49**, 4251 (1994).

<sup>5</sup>D. M. King *et al.*, Phys. Rev. Lett. **73**, 3298 (1994).

<sup>6</sup>A. J. Lowe, S. Regan, and M. A. Howson, Phys. Rev. B **44**, 9757 (1991).

<sup>7</sup>J.-S. Zhou, J. P. Zhou, J. B. Goodenough, and J. T. McDevitt, Phys. Rev. B **51**, 3250 (1995).

<sup>8</sup>T. Ami, M. K. Crawford, R. L. Harlow, Z. R. Wang, D. C. Johnston, Q. Huang, and R. W. Erwin, Phys. Rev. B **51**, 5994 (1995).

<sup>9</sup>J. C. Bonner and M. E. Fisher, Phys. Rev. **135**, A640 (1964).

<sup>10</sup>Z. Hiroi, M. Takano, M. Azuma, and Y. Takeda, Nature (London) **364**, 315 (1993).

<sup>11</sup>J. B. Goodenough, J.-S. Zhou, and J. Chan, Phys. Rev. B **47**, 5275 (1993).

<sup>12</sup>J. D. Jorgenson, B. Dabrowski, S. Pei, D. R. Richards, and D. G. Hinks, Phys. Rev. B **40**, 2187 (1989).

<sup>13</sup>C. Chaillout, J. Chenavas, S. W. Cheong, Z. Fisk, M. Marezio, B. Morosin, and J. E. Schirber, Physica C **170**, 87 (1990).

<sup>14</sup>J.-S. Zhou, H. Chen, and J. B. Goodenough, Phys. Rev. B **50**, 4168 (1994).

<sup>15</sup>J. B. Goodenough and A. Manthiram, J. Solid State Chem. **88**, 115 (1990).

<sup>16</sup>D. K. C. MacDonald, *Thermoelectricity: An Introduction to the Principles* (Wiley, New York, 1962).

<sup>17</sup>Y. J. Shin, E. D. Manova, J. M. Dance, P. Dordor, J. C. Grenier, E. Marquestaut, J. P. Doumerc, M. Pouchard, and P. Hagenmuller, Z. Anorg. Allg. Chem. **616**, 201 (1992).

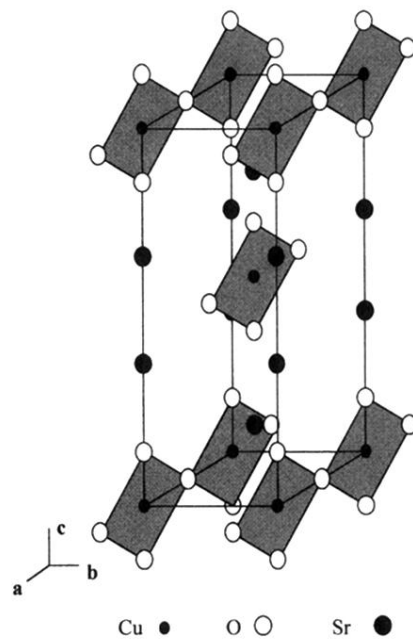


FIG. 1. The structure of orthorhombic  $\text{Sr}_2\text{CuO}_3$  showing isolated chains of corner-shared square-coplanar  $\text{CuO}_4$  units.